I. MOLECULAR TRANSFER OF NONEQUILIBRIUM NUCLEAR SPIN MAGNETIZATION

II. ELECTRON RESONANCE OF AN ORGANIC FREE RADICAL IN ZERO FIELD

Thesis by

Don D. Thompson

In Partial Fulfillment of the Requirements

for the Degree of

Doctor of Philosophy

California Institute of Technology

Pasadena, California

1960

ACKNOWLEDGEMENTS

It is with a great sense of gratitude that I acknowledge the aid of my research advisor, Dr. Harden M. McConnell, who has made my years at the Institute both profitable and very interesting. I am thankful for the opportunity to have associated with many other faculty members also, particularly Dr. Norman Davidson, and -- in my undergraduate years -- Dr. James Pitts.

I want to thank the Monsanto Chemical Corporation, the California Institute of Technology, and the U. S. Army Department of Ordnance for financial aid during my residency.

I acknowledge, with pride, the patience and understanding shown by my wife, Marilyn, who was willing to make great sacrifices so that this work might be done.

ABSTRACT

Part I contains a new magnetic resonance technique that has been developed to measure rates of fast molecular processes. The method involves the experimental introduction of a nonequilibrium nuclear magnetization in one system, A, and the subsequent measurement of the rate at which rapid molecular processes transfer this nonequilibrium magnetization to a second system, B. Systems A and B may correspond to different chemical sites in a molecule that give rise to a chemical shift, or to sites that are distinct because of electron coupled spin-spin interaction. This technique has been applied to determinations of the rate of proton exchange between ammonium ions in aqueous solution.

Part II contains a description of a theoretical and experimental investigation of zero field electron spin resonance of malonic acid radicals produced by X-irradiation at room temperature. The radicals produced in a single crystal are oriented in a specific manner. The theory involved predicts six lines of equal intensity, except for a very small Boltzmann factor. Some of these transitions have been found experimentally in a small modulation field at 77° K. The electron is presumed to "precess" in the field of the proton; however, the energy levels cannot be explained classically. A detailed account of the experimental apparatus is given.

INTRODUCTION

Since the advent of nuclear magnetic resonance (NMR) in 1946 and electron paramagnetic resonance (EPR) in 1945, a great many new and exciting discoveries in the field of chemistry have been made. In this comparatively short time, a host of vital information concerning molecular structure, crystal structure, and general kinetics has been forthcoming. A number of good textbooks and review articles are available (1)-(7) which describe in detail the theory and applications of these techniques. It is beyond the scope of this thesis to present these in a general way.

Only the theory that is generally connected with this research will be given a comprehensive treatment. Derivations and descriptions of apparatus that are not centered along the train of thought in the text are presented in the appendices.

TABLE OF CONTENTS

PART I

INTRODUCTION

The study of chemical reaction rates has been the subject of considerable interest to chemists for years, both theoretically and experimentally. With the advent of nuclear magnetic resonance (NMR) a new and very powerful tool for rate study was born. The progress of chemical reactions in solution may be followed if some characteristic of the observed spectrum changes during the course of the reaction. In cases where one of the reactants or one of the products of reaction shows characteristic fine structure, observation of the strength of resonance associated with a particular molecular grouping may afford a means of observing the progress of the reaction.

In other cases the thermal, or longitudinal, relaxation time, T_1, may change as the reaction proceeds. This also affords a method to follow the reaction by successive T_1 measurements. T_1 is defined as one-half the mean transition probability for spin up and spin down "quantum jumps" for nuclei whose spin is 1/2 and similarly for nuclei whose spin is greater than 1/2. An alternate definition of T_1 is given by Bloch (1). This definition states that T_1 is the time for the microscopic magnetization to return to $\frac{1}{e}$ of its original value after being

tilted in the act of resonance. Hickmott and Selwood (8) used this method to follow the reduction of Eu^{+3} to Eu^{+2} in dilute hydrochloric acid solution.

Relaxation time studies may also be employed in the study of solid paramagnetic catalysts for reactions in the liquid state. The catalytic activity depends on the accessibility of the paramagnetic ions to the molecules of the liquid. A study of the variation of T_1 with catalyst concentration will provide information concerning the structure and mechanism of the catalyst (9).

Chemical exchange is another phenomenon that lends itself easily to study by NMR or EPR. Several interesting studies concerning proton or electron exchange have been completed. The work of Meiboom et al. (10), on the alkyl ammonium ions, is indicative of the type of research that is being conducted in this field. If protons are being transferred between two chemical entities the resulting NMR spectrum is dependent upon the rate of the process. When the rate is very slow the spectrum shows two unequivalent lines; if the rate is very fast, the lines merge and an "average" line is produced. A study of the broadening produced by the uncertainty of the proton's magnetic environment may yield a suitable rate constant for the process.

The purpose of this section is to present a new effect whereby rapid molecular processes, such as exchange, may be measured from the spectra of the compounds involved. This complete study is given elsewhere (11). Qualitatively, the idea may be expressed in the following manner. If one has a nuclear specie in one of two distinct magnetic environments, A and B, and one visualizes some rapid process whereby these two identical nuclei change environments, then if nonequilibrium nuclear spin magnetization is produced in A, it may be transferred to B. The spin magnetization can be placed in A by an adiabatic rapid passage experiment. This magnetization will be transferred, if the spin-lattice relaxation time, T_1, is greater than the lifetime of transfer, (τ). Hence, nonequilibrium spin magnetization produced in A may appear in B at some later time depending upon the relaxation times in A and B and the lifetime of transfer.

To test this hypothesis, the system of saturated acidified aqueous ammonium nitrate was chosen. Using this system one may use conventional NMR techniques to measure the rate (12), and compare this to the proposed method. In this solution, two proton exchanges are possible. One exchange is between ammonium ions and water and the other between like ammonium ions. For solutions of pH less than 2.5, exchanges between water and ammonium ions can be neglected, as will be shown later. One need only consider proton exchange between ammonium ions, which is presumably catalyzed by

ammonia molecules(12). The conventional method discussed in the introduction was used(13) to measure the rate of proton exchanges in the solutions where exchanges with water may be neglected. This method involves collapse of the multiplets associated with the H^1-N^{14} spin-spin interactions. The rate constants so obtained were then used to calculate the rate of transfer of nonequilibrium nuclear spin magnetization from one ion to another (with different N^{14} nuclear spin orientations) by means of rapid passage experiments (1). In the first section of the following theory, the conventional NMR experiments used to obtain the rate constants for exchanges between ions will be described. The second section will describe the theory involved in the transfer of nonequilibrium nuclear spin magnetization.

Theory

1. Proton Exchange Rates

Figures 1(a), 1(b), and 1(c) illustrate the effect of changing the pH from 1.0 to 2.5 for saturated aqueous ammonium nitrate solution. It will be observed that the ammonium ion proton triplet shows marked broadening (from 3 sec^{-1} to about 40 sec^{-1}) over this pH range. At precisely pH = 2.35 the lines are so broad that they are not discernible, whereas the water line is still only 10 sec^{-1} wide. In highly acid solutions where there is essentially no exchange, the proton line width for water is only 2.8 sec^{-1}. In Fig. 1(c), it is seen that at pH = 2.5

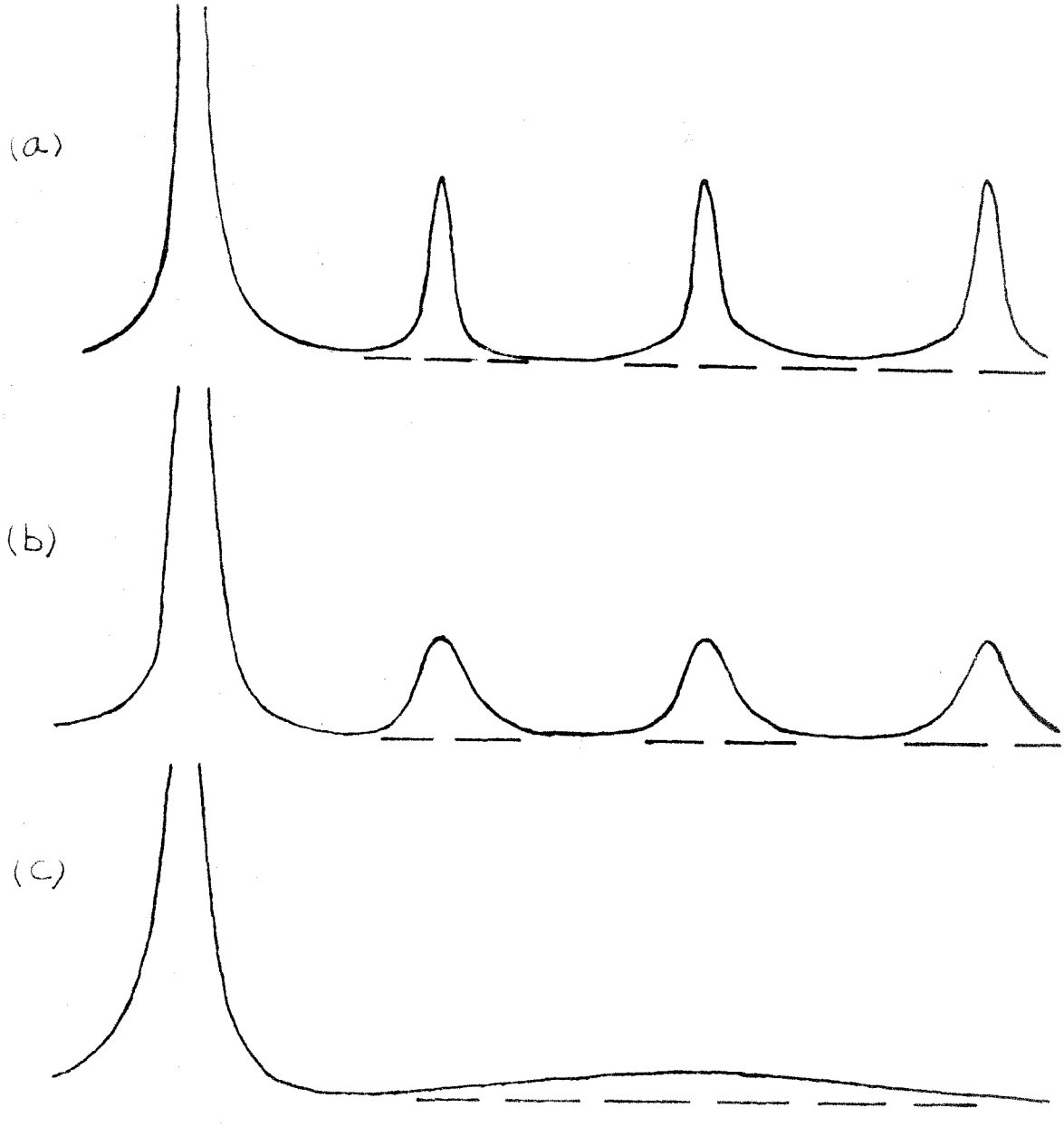

Figure 1. - Effect of pH on ammonium ion resonance. (a) pH = 1.0; (b) pH = 1.5; (c) pH = 2.5. The strong signal at the left is due to water. The spin-spin splittings in (a) are 51 ± 1 sec^{-1}.

the ammonium lines reappear but the triplet has collapsed into a single broad line about 60 sec^{-1} wide. The water line stays approximately 10 sec^{-1} wide. Under these conditions there is rapid exchange of protons among ammonium ions but the rate of proton exchange between the ions and water is still comparatively slow. In the pH range 2.55 to 3.3, the line of water increases rapidly and the lines for all protons begin to overlap. At pH = 3.3, there is only one line in the entire spectrum and it is about 75 sec^{-1} wide. From pH = 3.3 to 5.5 the single line narrows to 3 sec^{-1}. Under these conditions, of course, proton exchanges between all species are very rapid. From these data it was concluded that at a pH of 1.5 the proton exchange with water could be neglected in an experiment on transfer of nonequilibrium nuclear spin magnetization. It was, therefore, at this pH that an effort was made to obtain the rate of proton exchange between ammonium ions with some accuracy. The method used to analyze line shapes was that of Gutowsky, McCall, and Slichter (13), as modified to include the case of three equally probable magnetic environments corresponding to the three almost equally probable orientations of the N^{14} nuclear spin. The calculations were first carried out by using the method of GMS, and later using the method of McConnell (14). The results are identical. The theoretical spectrum (see Fig. 2) corresponds to a proton lifetime of 0.06 sec. The general theoretical equation, using the nomenclature of GMS for the calculated line shape in Fig. 2 is

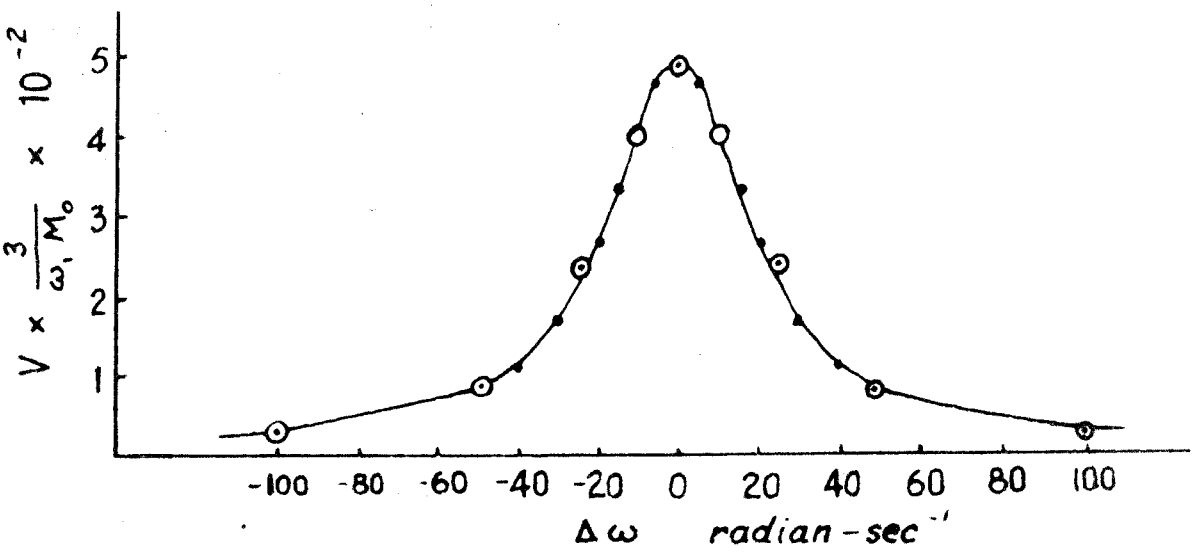

Figure 2. - Calculated and observed line shapes for one multiplet signal; O calculated, O observed.

$$G = -\frac{\omega_1 Mo}{3}\left[\frac{A + iB}{C + iD}\right]$$

where

$$A = 36\tau\Delta\omega + \frac{24\tau^2\Delta\omega}{T_2}$$

$$B = 27 + \frac{36\tau}{T_2} + \frac{12\tau^2}{T_2^2} - 12\tau^2(\Delta\omega)^2 + 4\tau^2\left(\frac{\delta\omega}{2}\right)^2$$

$$C = \frac{9}{T_2} + \frac{12\tau}{T_2^2} - 12\tau(\Delta\omega)^2 + 4\tau\left(\frac{\delta\omega}{2}\right)^2 + \frac{4\tau^2}{T_2^3} \qquad (1)$$

$$- 12\tau^2\frac{(\Delta\omega)^2}{T_2} + \frac{4\tau^2}{T_2}\left(\frac{\delta\omega}{2}\right)^2$$

$$D = -9\Delta\omega - \frac{24\tau\Delta\omega}{T_2} - \frac{12\tau^2\Delta\omega}{T_2^2} + 4\tau^2(\Delta\omega)^3$$

$$- 4\tau^2\Delta\omega\left(\frac{\delta\omega}{2}\right)^2$$

The constants T_2, τ have values 0.21 and 0.06 sec., respectively, and these "values" give the calculated spectrum in Fig. 2. The lifetime τ (and the rate constant k) refers to proton transfers between ammonium ions with different N^{14} nuclear spin orientations. The lifetime of transfer between <u>any</u> ion is 2/3 τ and the corresponding rate constant is 3/2 k.

2. Transfer of Nonequilibrium Nuclear Spin Magnetization

In this section, we consider what is involved when one observes the rapid passage nuclear magnetic resonance spectrum of the ammonium ion. As indicated in the previous section, one completely neglects the effect of exchange of protons with the water molecules. Consider that an individual proton with nuclear spin $I = 1/2$ can be in one of six possible "states." The proton can be in a magnetic environment A with spin up; it can be in magnetic environment A with spin down; it can be in magnetic environment B with spin down; it can be in magnetic environment B with spin up, etc. The possible magnetic environments A, B, C, in which a proton can be situated correspond to the three possible internal magnetic fields acting at a proton due to the spin-spin interaction with N^{14}. Let N_+^A be equal to the number of protons in state A with spin up and let N_+^0 be the number of spins in A (or B, or C) under equilibrium conditions. The quantities N_-^A, N_+^B, etc., are defined similarly. The various possible "states" for the proton with spin 1/2 are shown in Fig. 3, which shows also the appropriate instantaneous number of spins in the various states. The differential equations governing the rate of change of the number of spins in the various states are illustrated below for N_+^A and N_-^A.

$$\dot{N}_+^A = -T_1^{-1}(N_+^A - N_+^0) - k(N_+^A - N_+^B) - k(N_+^A - N_+^C) \quad (2)$$

$$\dot{N}_-^A = -T_1^{-1}(N_-^A - N_-^0) - k(N_-^A - N_-^B) - k(N_-^A - N_-^C). \quad (3)$$

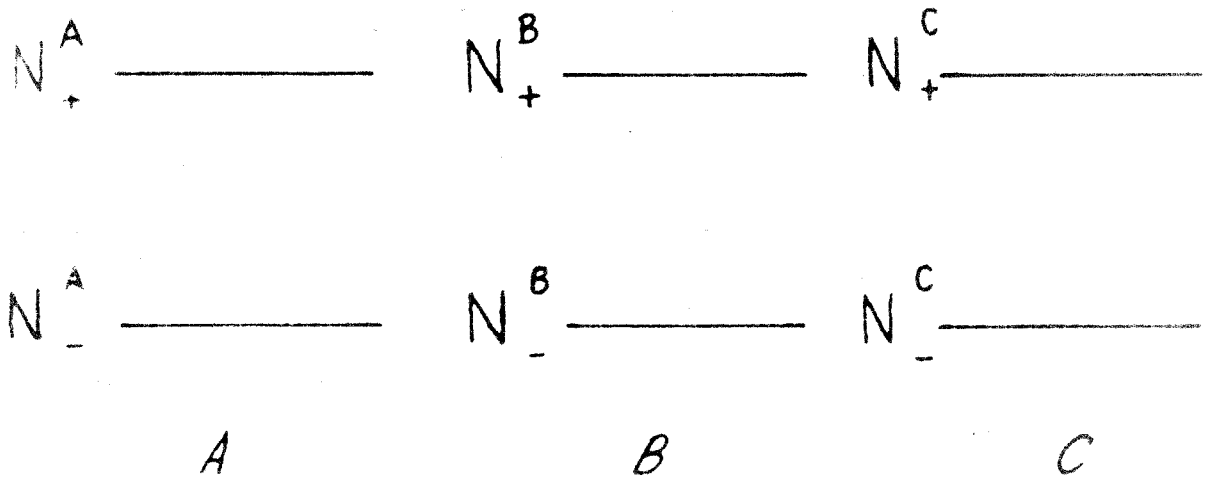

Figure 3. - The six possible states for a proton in three magnetic environments.

In the preceding equations k gives the specific rate constant for proton transfer between environments A and B. It may be noted that in formulating the kinetic equations (2) and (3), it has been assumed the proton does not relax ("flip") in the transfer process. This is a most plausible assumption as long as the intermediate (NH_3, for example) is very short-lived and is nonparamagnetic. One may introduce the notation

$$\delta^A = N_+^A - N_-^A , \tag{4}$$

$$\delta^0 = N_+^0 - N_-^0 , \tag{5}$$

and obtain the abbreviated equations,

$$\dot{\delta}^A = -T_1^{-1}(\delta^A - \delta^0) - k(\delta^A - \delta^B) - k(\delta^A - \delta^C) , \tag{6}$$

or

$$\dot{\delta}^A = -(T_1^{-1} + 2k)\delta^A + T_1^{-1}\delta^0 + k(\delta^B + \delta^C) , \tag{7}$$

$$\dot{\delta}^B = -(T_1^{-1} + 2k)\delta^B + T_1^{-1}\delta^0 + k(\delta^A + \delta^C) , \tag{8}$$

$$\dot{\delta}^C = -(T_1^{-1} + 2k)\delta^C + T_1^{-1}\delta^0 + k(\delta^A + \delta^B) . \tag{9}$$

Defining $\Delta = \delta^A + \delta^B + \delta^C$ and $\Delta^0 = 3\delta^0$, then from (7)-(9) you obtain

$$\dot{\Delta} = -T_1^{-1}(\Delta - \Delta^0) , \tag{10}$$

$$\dot{\delta}^A - \dot{\delta}^B = -(T_1^{-1} + 3k)(\delta^A - \delta^B) , \tag{11}$$

$$\dot{\delta}^B - \dot{\delta}^C = -(T_1^{-1} + 3k)(\delta^B - \delta^C) . \tag{12}$$

The solutions of these simple first-order homogeneous linear differential equations are

$$\Delta - \Delta^0 = (\Delta - \Delta^0)_i \exp(-t/T_1) , \tag{13}$$

$$\delta^A - \delta^B = (\delta^A - \delta^B)_i \exp(-[T_1^{-1} + 3k]t) , \tag{14}$$

$$\delta^B - \delta^C = (\delta^B - \delta^C)_i \exp(-[T_1^{-1} + 3k]t) , \tag{15}$$

where the subscript i indicates the initial values of these quantities at t = 0. Equations (13)-(15) can be solved for δ^A, δ^B, and δ^C.

$$\delta^A = \delta^0 + \frac{1}{3}[2\delta^A - \delta^B - \delta^C]_i \exp(-[T_1^{-1} + 3k]t) + \frac{1}{3}[\delta^A + \delta^B + \delta^C - 3\delta^0]_i \exp(-t/T_1) , \tag{16}$$

$$\delta^B = \delta^0 + \frac{1}{3}[2\delta^B - \delta^A - \delta^C]_i \exp(-[T_1^{-1} + 3k]t) + \frac{1}{3}[\delta^A + \delta^B + \delta^C - 3\delta^0]_i \exp(-t/T_1) , \tag{17}$$

$$\delta^C = \delta^0 + \frac{1}{3}[2\delta^C - \delta^A - \delta^B]_i \exp(-[T_1^{-1} + 3k]t) + \frac{1}{3}[\delta^A + \delta^B + \delta^C - 3\delta^0]_i \exp(-t/T_1). \tag{18}$$

Let λ be the time taken in going from the center of one resonance signal to the center of the next resonance signal. Let 2ϵ be the time spent in going through one resonance signal. In the present calculations

we assume that $2\epsilon \ll \tau$, although this condition is not ideally realized in all of our experiments. We shall use the following time scale to develop our mathematical discussion. At time $t = -\epsilon$ you enter into the A resonance signal. At time $t = 0$ you are in the center of the A signal, and at time $t = \epsilon$ you have passed the A signal. At time $t = \tau\lambda - \epsilon$ you enter the resonance of B, $t = \tau\lambda$ corresponds to the center of the B resonance, and at time $t = \tau\lambda + \epsilon$ you have passed the B resonance. Similarly, $t = 2\tau\lambda$ corresponds to the center of the C resonance, and the times $t = 2\tau\lambda - \epsilon$ and $2\tau\lambda + \epsilon$ represent times of entering and leaving the C resonance.

Equations (16)-(18) can be used to calculate the spin magnetization at any particular time.

At time $t = -\epsilon$,

$$\sigma^A = \sigma^0 ,$$

$$\sigma^B = \sigma^0 ,$$

$$\sigma^C = \sigma^0 . \qquad (19)$$

At time $t = \epsilon$,

$$\sigma^A = \sigma^0 \cos\theta ,$$

$$\sigma^B = \sigma^0 ,$$

$$\sigma^C = \sigma^0 . \qquad (20)$$

One now uses the σ values in (20) to calculate the "initial" terms in (16)-(18) for time $t = \lambda - \epsilon$. Thus, at time $t = \lambda - \epsilon$, you have

$$\delta^A = \delta^0 + \frac{1}{3}[2\delta^0(\cos\theta - 1)]\exp(-[T_1^{-1} + 3k]\lambda)$$

$$+ \frac{1}{3}\delta^0(\cos\theta - 1)\exp(-\lambda T_1^{-1}), \quad (21)$$

$$\delta^B = \delta^0 + \frac{1}{3}[\delta^0(1 - \cos\theta)]\exp(-[T_1^{-1} + 3k]\lambda)$$

$$+ \frac{1}{3}\delta^0(\cos\theta - 1)\exp(-\lambda T_1^{-1}). \quad (22)$$

$$\delta^C = \delta^0 + \frac{1}{3}[\delta^0(1 - \cos\theta)]\exp(-[T_1^{-1} + 3k]\lambda)$$

$$+ \frac{1}{3}\delta^0(\cos\theta - 1)\exp(-\lambda T_1^{-1}). \quad (23)$$

Note that in the preceding equations $\lambda - \epsilon$ has been approximated by λ.

At time $t = \lambda$ you therefore expect a peak resonance signal proportional to the value of δ^B given in (22).

At time $t = \lambda + \epsilon$, after the B resonance has been traversed, the B magnetization will have been tilted through an angle of θ. Thus, at time $t = \lambda + \epsilon$,

$$\delta^A = \text{same as in (21)}. \quad (24)$$

$$\delta^B = \delta^0\cos\theta + \frac{1}{3}\cos\theta\,[\delta^0(1 - \cos\theta)\exp(-[T_1^{-1} + 3k]\lambda)]$$

$$+ \frac{1}{3}\delta^0\cos\theta\,(\cos\theta - 1)\exp(-\lambda T_1^{-1}), \quad (25)$$

$$\delta^C = \text{same as in (23)}. \quad (26)$$

The next step is the calculate $\mathcal{S}^C$ at the time $t = 2\lambda$, since the value of $\mathcal{S}^C$ at this time will be proportional to the observed signal. You may do this by taking $\mathcal{S}^A$, $\mathcal{S}^B$, and $\mathcal{S}^C$ in (24)-(26) as initial values in (16)-(18) and setting $t = \lambda$ in (16)-(18). The value of $\mathcal{S}^C$ obtained thereby is given in the following equation:

$$\mathcal{S}^C = \mathcal{S}^0 + \frac{1}{3}\mathcal{S}^0 (\cos\theta - 1) \exp(-\lambda T_1^{-1}) [1 - \exp(-3k\lambda)]$$

$$\times [\frac{1}{3} \exp(-\lambda T_1^{-1}) [1 - \exp(-3k\lambda)] (\cos\theta + 1)$$

$$+ \frac{2}{3} \exp(-\lambda T_1^{-1}) [1 + 2 \exp(-3k\lambda)]]. \qquad (27)$$

In the foregoing work it is, of course, assumed that the time spent on resonance - that is, the time spent in passing through a typical broad fast-passage resonance - is small compared to the time λ, spent in going from one resonance to another one. It may also be noted that one should assume that the resonance intensities are proportional to the $\mathcal{S}$ values when a resonance is begun. The basic requirement here is that the transfer process give rise to no transverse nuclear spin magnetization. For example, when the spin magnetization in environment A is turned upside down, this nonequilibrium magnetization moves into the B system, but there will be no transverse magnetization in the B system, although there may be transverse magnetization in the A system after the pulse at A, because the transverse

magnetization moves from the A system into the B system at different times and if the precession frequency of nuclear spin magnetization in the A system is fast compared to the rate of transfer of nuclear spin magnetization from the A system to the B system, then there will be no transverse nuclear spin magnetization in the B system. Hence, the resonance intensities in the B system will be proportional to the nuclear spin magnetization in the B system in the field direction.

Figure 4 is a typical high to low field rapid passage spectrum for which $\theta = 180°$. One can demonstrate that $\theta = 180°$ to within experimental error by showing the high to low field spectrum to be the negative (inverse) of the low to high field spectrum. This complete inversion was obtained for the spectrum in Fig. 4 and for all other spectra used in the calculation of intensity ratios.

Experimental

1. Chemicals

The ammonium nitrate was reagent grade and no further attempt was made to purify it. The nitric acid added to acidify the solutions was from laboratory stock. The solutions were stored in polyethylene containers, as their pH was found to change in glass if stored for over a week. The samples were sealed off in 5 mm pyrex tubing for insertion into the instrument. It was found that the exclusion of oxygen was unnecessary. At room temperature a saturated solution of ammonium

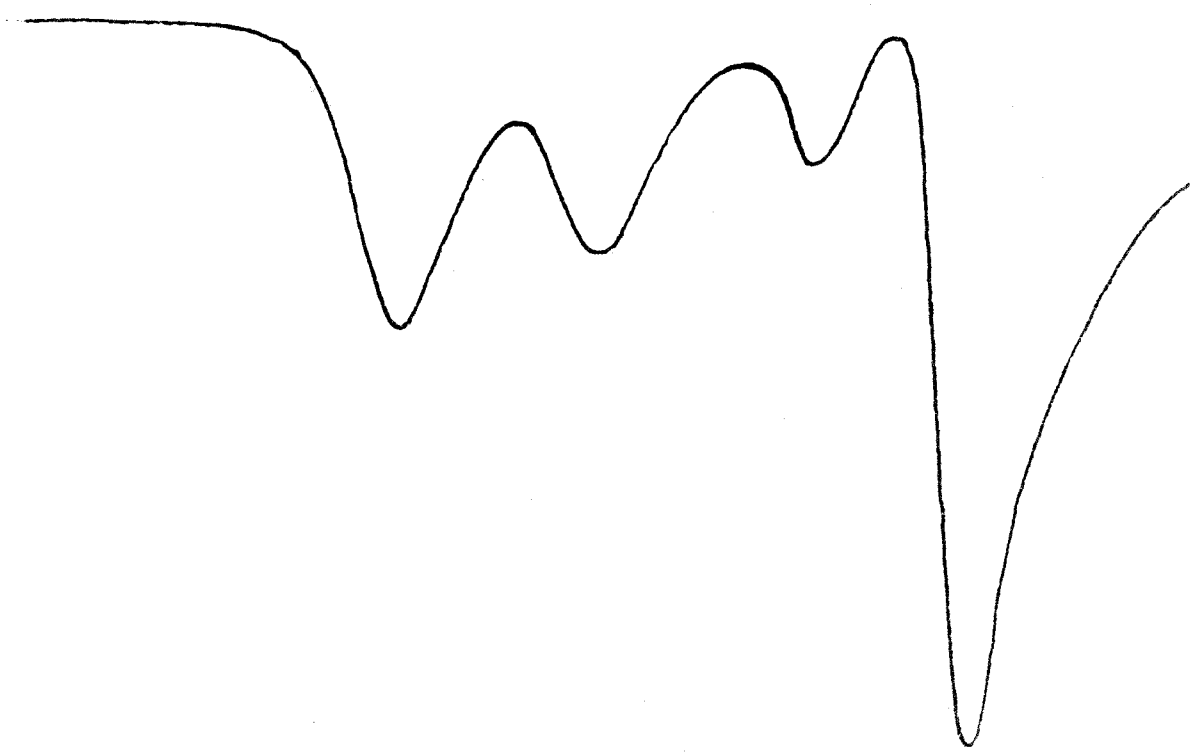

Figure 4. - Tracing of oscillogram showing the spectrum under conditions of "fast passage," dispersion mode, and sweep from high to low applied field.

nitrate is about 10.8 M. The small quantities of acid added did not affect the solubility appreciably.

2. Apparatus

A Beckman laboratory model pH meter was used to make the solutions of known acidity. The NMR spectrometer was a Varian Associates V-4300, high resolution unit with a 12" magnet, operating at fixed peak frequency of 40 Mc. The T_1 measurements were made with the aid of a Hewlett-Packard model 202A function generator. See Appendix III for details of the T_1 measurements.

In order to see the predicted intensity decrements the pH = 1.5 solution was inserted into the instrument and it was tuned to dispersion mode with high power. When complete signal inversion was obtained ($\theta = 180°$) for high to low field sweep, photographs of the oscilloscope tracings were made. The sweep was much too fast for recording. The integrated intensity ratios for this solution are then to be compared to those predicted from equations 22 and 27.

Results

In Fig. 4 the sweep rate corresponds to $\lambda = 0.41$ sec. In this and several similar experiments the average integrated intensity ratios for the three signals are 1.0:0.8:0.6. In the theoretical equations 22 and 27, the intensity ratios depend on θ, $\exp(-\lambda k)$, and $\exp(-\lambda T_1^{-1})$. In the experiment performed $\theta = 180°$, $\exp(-\lambda k)$ is negligible in

equations 22 and 27, and $\exp(-\gamma T_1^{-1})$ is ~ 0.37. The values for the experimental parameters together with equations 22 and 27 yield the theoretical intensity ratios 1.0:0.75:0.70. Everything considered, this calculation is in good accord with the observed ratios.

In many other experiments with fast sweeps under conditions where $\gamma T_1^{-1} \ll 1$, the visually estimated intensity ratios approximated those given by equations 22 and 27 for this fast sweep limit, i.e., 1:1/3:1/9. Difficulties associated with photographing these rapid sweeps prevented quantitative fast sweep measurements. At a pH = -0.4 experiments that were otherwise identical to those previously described were carried out, and the observed rapid passage spectra showed no intensity decrements in the spin-spin multiplets whatsoever. In this work T_2 was taken from a line width measurement of the same solution. It was found that calculated line shapes such as those illustrated in Fig. 2 were relatively insensitive to possible small errors in T_2.

Conclusion

It should be pointed out here that the accuracy of this new method for finding rates of rapid molecular processes is only of the order of 10% for most cases; however, for many rate studies this is sufficient. Several other systems would lend themselves to this type treatment. The best feature of this method is the simplicity with which one may

calculate the rates. The only additional data needed here in excess of data for a GMS type calculation are the experimental intensity ratios and the sweep time, λ , both of which are easily obtained. A T_1 measurement is needed for both methods.

It should be noted here that an actual rate determination was not made on this or any other system. The calculated rate was identical with that of Meiboom et. al. (10), and the equivalence of the experimental data with that predicted theoretically is a point in fact. This method of rate determination is somewhat more limited than that of GMS, but for specific cases is a much easier method.

PART II

INTRODUCTION

The rupture of chemical bonds by radiation in the ultra-violet region, or by X- or γ-rays, is one of the most general and direct methods for producing fragmented molecules or free radicals. The bonds between atoms can often be broken by these irradiations, and the minimum energy required is just the energy of the bond itself. Most bond strengths are about 4 to 10 electron volts in energy and this corresponds to wavelengths in the ultra-violet region. However, in order to hinder the subsequent recombination of the fragments, it is sometimes necessary to provide a high viscosity medium. The matrix usually employed is kept at low temperatures to insure the radicals' long life. Certain substances when irradiated in the solid state at room temperature will exhibit paramagnetism for hours, even months. Malonic acid is one of these substances (16). When X-rays are employed, there is sufficient energy imparted to the fragment that it will move through the matrix and be less likely to recombine.

The first EPR spectra from active radicals formed by ultra-violet irradiation and trapped at low temperatures were obtained by Ingram et al. (2). In these experiments the compounds under study were dissolved in hydrocarbons and the solutions were then frozen

at liquid nitrogen temperatures (77° K) to form rigid glasses. The temperature of the glass may be altered by heating and a study of the effect of the viscosity change made upon the radical.

Spectra of organic radicals produced by irradiations may be placed somewhat uniquely into two groups. In the first group the radicals produced undergo rapid isotropic tumbling motions. This tumbling usually occurs in solutions, or glasses, of low viscosity. Sometimes tumbling occurs even in rigid mediums. The spectra of these rapidly tumbling radicals usually are easily interpreted in terms of isotropic coupling constants (17).

The second group of radicals consists of those whose orientation is known from crystallographic information. Proton hyperfine splittings (hfs) of these radicals are a combination of the Fermi isotropic coupling and the anisotropic dipolar (electron-spin - proton-spin) interaction. These two interactions are sometimes of the same order of magnitude. The interpretation of spectra of this type may be very difficult; however, they yield additional information concerning molecular structure that cannot be obtained from a freely tumbling molecule. Polycrystalline samples or glasses are generally poor for interpreting anisotropies because of the inherent line broadening produced by this anisotropy. For a really meaningful analysis of anisotropic splittings a single crystal is employed where a definite orientation of the radical may be produced.

The first significant work on oriented free radicals was done by McConnell, Heller, Cole, and Fessenden (18). These authors used single crystals of malonic acid which were X-rayed to produce an R_2CH radical. Here the R refers to -COOH.

Malonic acid is triclinic (19) with $a = 5.33$ Å, $b = 5.14$ Å, $c = 11.25$ Å, $\alpha = 102°42'$, $\beta = 135°10'$, $\gamma = 85°10'$. The unit cell contains two molecules which are related by a center of symmetry (see Fig. 5).

McConnell et al. used the following spin Hamiltonian to describe the EPR of the R_2CH oriented radical:

$$\hat{H} = \hat{H}_z + \hat{H}_{hf} \tag{28}$$

where H_z was also shown to be nearly equal to

$$h\nu_e S_H - h\nu_p I_H$$

ν_e and ν_p are the resonance frequencies of the electron and proton respectively and S_H and I_H are their respective spin angular momenta along the field direction. The authors showed that the Hamiltonian for hfs can be expressed in the following manner:

$$\hat{H}_{hf} = hA\hat{S}_z\hat{I}_z + hB\hat{S}_x\hat{I}_x + hC\hat{S}_y\hat{I}_y \tag{29}$$

where A, B, and C are terms containing both the isotropic and anisotropic coupling constants. Thus,

$$\begin{aligned} A &= A_d + a \\ B &= B_d + a \\ C &= C_d + a \end{aligned} \tag{30}$$

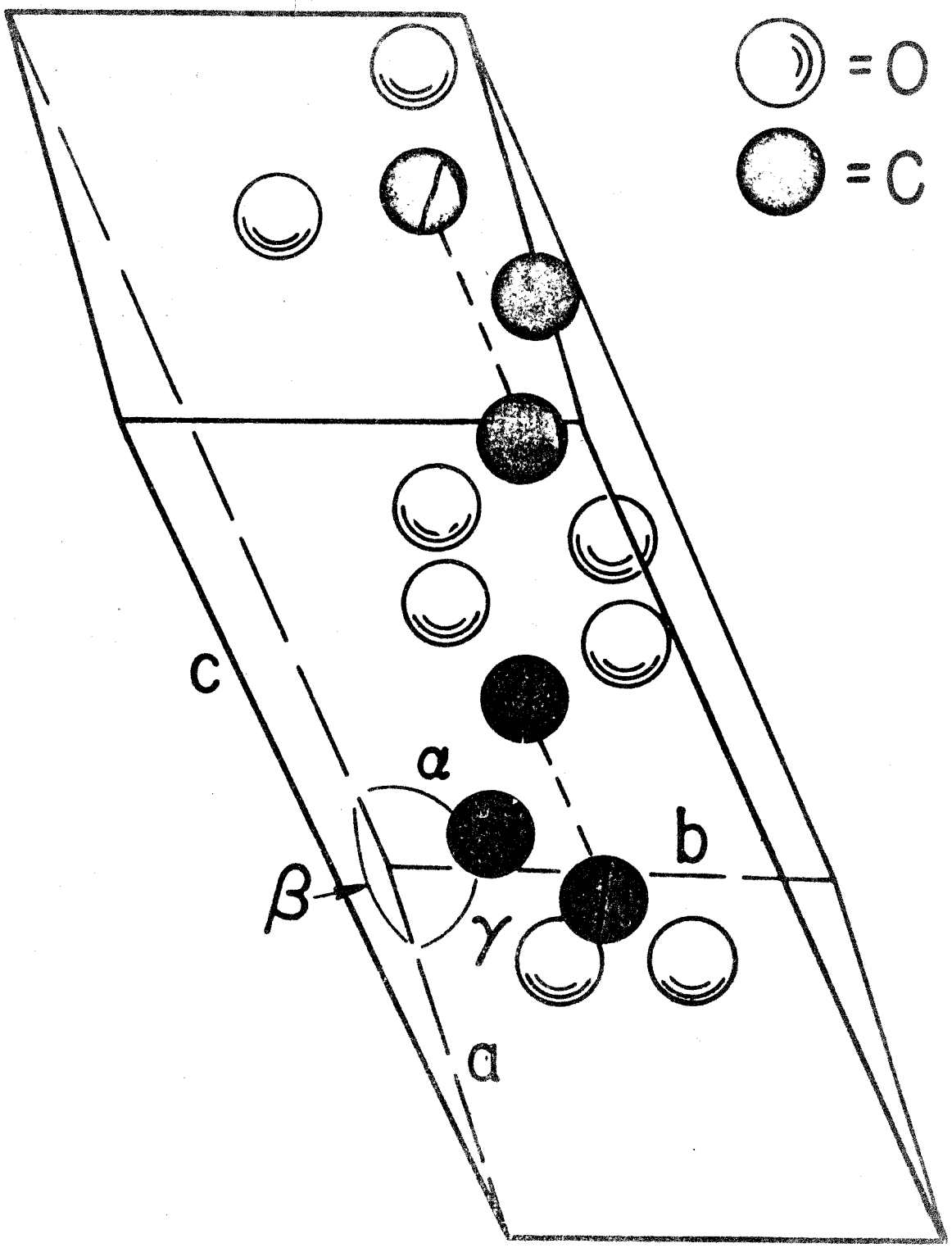

Figure 5. - A diagram showing the unit cell of malonic acid. The cell constants are given in the text.

where a is the isotropic coupling constant and A_d, B_d, and C_d are the dipolar contributions. The sum of A_d, B_d, and C_d is equal to zero and therefore from an experimental measurement of A, B, and C, all of the quantities can be calculated. Their values are:

$$A = -29 \pm 2 \text{ Mc.}$$

$$B = -61 \pm 2 \text{ Mc.}$$

$$C = -91 \pm 2 \text{ Mc.}$$

Using the Hamiltonian (29) it is possible to describe the hfs states of R_2CH in zero applied field. The purpose of this part of the thesis is to describe in detail the study, both theoretically and experimentally, of R_2CH in zero field.

Theory

Figure 6 is a drawing of the planar R_2CH radical. The z axis of a rectangular cartesian coordinate system lies along the molecular C-H bond axis. Equation (29) may be written in the following manner:

$$\underset{\wedge}{H} = hA \underset{\wedge}{S}_z \underset{\wedge}{I}_z + 1/4\, h(B + C)[\underset{\wedge}{S}_+ \underset{\wedge}{I}_- + \underset{\wedge}{S}_- \underset{\wedge}{I}_+] \qquad (31)$$

$$+ 1/4\, h(B - C)[\underset{\wedge}{S}_+ \underset{\wedge}{I}_+ + \underset{\wedge}{S}_- \underset{\wedge}{I}_-]$$

by substituting in equation (29) the following definitions of the spin raising and lowering operators S_+ and S_-:

$$\underset{\wedge}{S}_+ = \underset{\wedge}{S}_x + i\, \underset{\wedge}{S}_y$$

$$\underset{\wedge}{S}_- = \underset{\wedge}{S}_x - i\, \underset{\wedge}{S}_y$$

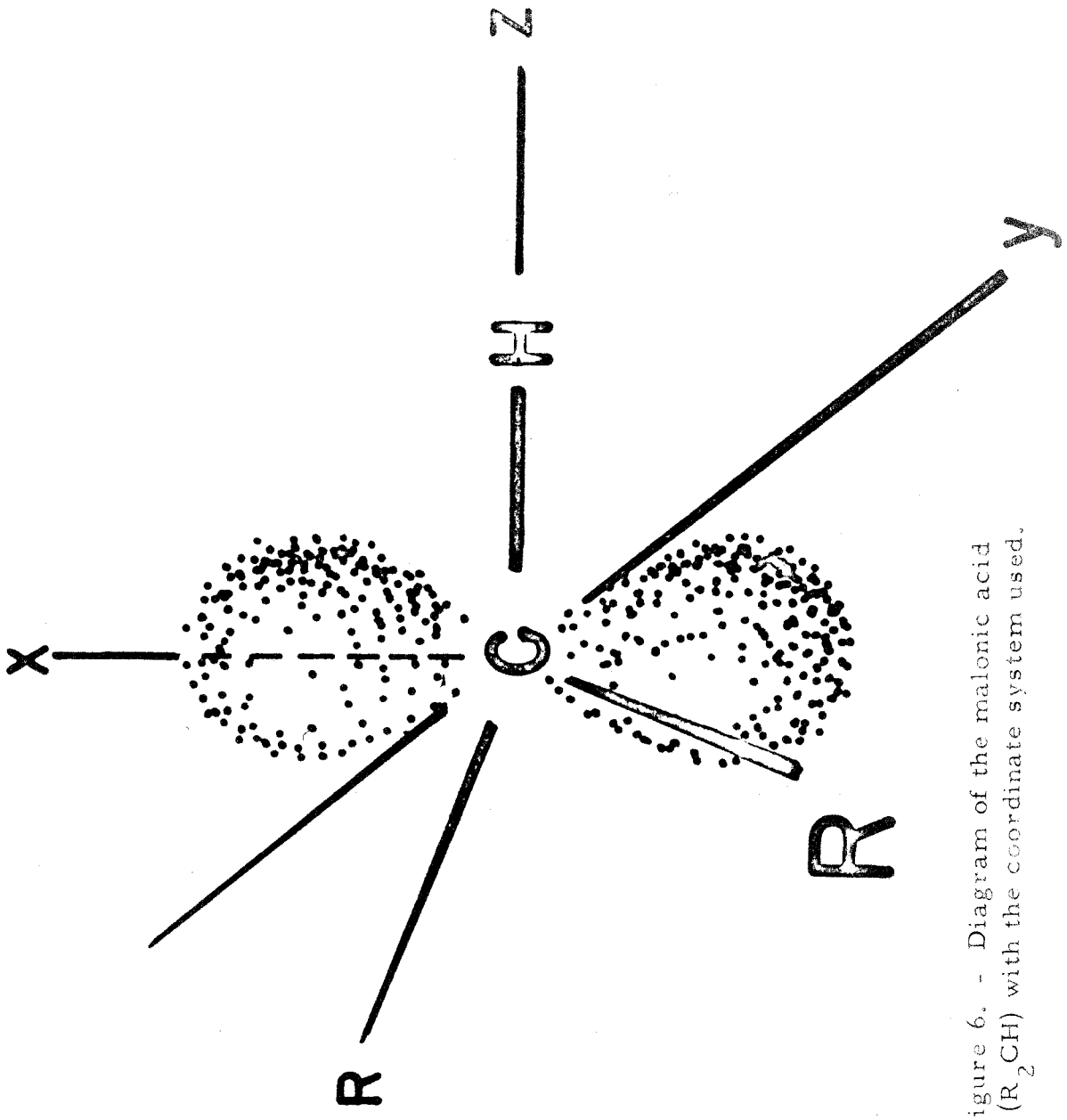

Figure 6. - Diagram of the malonic acid radical (R_2CH) with the coordinate system used.

The corresponding eigenfunctions of equation (31) are:

$$\Psi_1^0 = \frac{1}{\sqrt{2}} \left[\alpha(e)\,\alpha(p) + \beta(e)\,\beta(p) \right]$$

$$\Psi_2^0 = \frac{1}{\sqrt{2}} \left[\alpha(e)\,\alpha(p) - \beta(e)\,\beta(p) \right] \qquad (32)$$

$$\Psi_3^0 = \frac{1}{\sqrt{2}} \left[\alpha(e)\,\beta(p) + \beta(e)\,\alpha(p) \right]$$

$$\Psi_4^0 = \frac{1}{\sqrt{2}} \left[\alpha(e)\,\beta(p) - \beta(e)\,\alpha(p) \right]$$

These functions are linear combinations of the spin up (α) and spin down (β) functions of the electron and proton contained in the non-interacting CH fragment. The corresponding zero-field eigenenergies are:

$$E_1^0 = \frac{1}{4}A + \frac{1}{4}(B-C) = 0.3 \text{ Mc.}$$

$$E_2^0 = \frac{1}{4}A - \frac{1}{4}(B-C) = -14.7 \text{ Mc.} \qquad (33)$$

$$E_3^0 = -\frac{1}{4}A + \frac{1}{4}(B+C) = -31.0 \text{ Mc.}$$

$$E_4^0 = -\frac{1}{4}A - \frac{1}{4}(B+C) = 45.0 \text{ Mc.}$$

with the A, B, and C given in megacycles. Figure 7 is a drawing of the energy level diagram for this system.

In the absence of an applied field there are, of course, no "π" or "∂" transitions as are usually encountered in studying Zeeman levels. The transitions considered here are with respect to the direction of the applied RF field, and an X transition, for example,

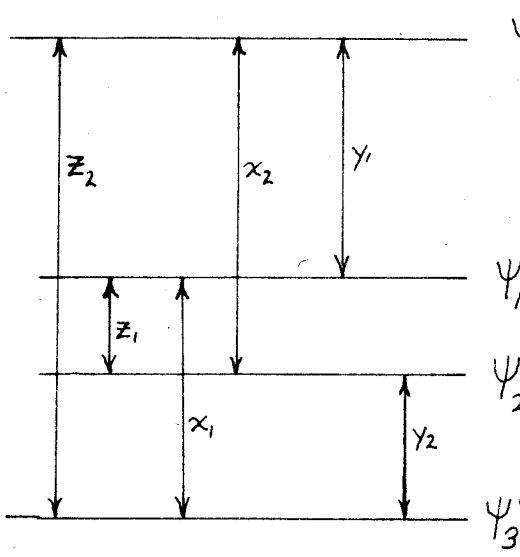

$X_1 = 30.7$ Mc. $\quad Y_1 = 45.3$ Mc. $\quad Z_1 = 15.0$ Mc.

$X_2 = 59.7$ Mc. $\quad Y_2 = 16.3$ Mc. $\quad Z_2 = 16.3$ Mc.

$$E_1^\circ = -\tfrac{1}{4}A + \tfrac{1}{4}(B-C) \qquad E_2^\circ = \tfrac{1}{4}A - \tfrac{1}{4}(B-C)$$

$$E_3^\circ = -\tfrac{1}{4}A + \tfrac{1}{4}(B+C) \qquad E_4^\circ = -\tfrac{1}{4}A - \tfrac{1}{4}(B+C)$$

Figure 7. - Energy level diagram for malonic acid radical in zero applied field.

is one in which the x direction in Fig. 6 is placed along the coil axis. One needs to calculate the dipole moment matrix elements of the type

$$\left(\psi_i^0 \left| \underset{\wedge}{\mu}_x \right| \psi_j^0\right) \tag{34}$$

to determine the relative transition probabilities. The transition probability will be proportional to the square of these matrix elements. The operator μ is given by the following expression:

$$\underset{\wedge}{\mu} = g_0 \, \beta \, \underset{\wedge}{S} \tag{35}$$

where g_0 and β are respectively the spectroscopic splitting factor and the Bohr magneton. Using the above equations one calculates that there are six possible transitions, two in the x direction and two each in the y and z directions. The corresponding transition probabilities are proportional to

$$\begin{aligned}
\left|(\psi_1^0 \left| \underset{\wedge}{\mu}_x \right| \psi_3^0)\right|^2 &= 1/4 \, g_0^2 \, \beta^2 \\
\left|(\psi_2^0 \left| \underset{\wedge}{\mu}_x \right| \psi_4^0)\right|^2 &= 1/4 \, g_0^2 \, \beta^2 \\
\left|(\psi_1^0 \left| \underset{\wedge}{\mu}_y \right| \psi_4^0)\right|^2 &= 1/4 \, g_0^2 \, \beta^2 \\
\left|(\psi_3^0 \left| \underset{\wedge}{\mu}_y \right| \psi_2^0)\right|^2 &= 1/4 \, g_0^2 \, \beta^2 \\
\left|(\psi_2^0 \left| \underset{\wedge}{\mu}_z \right| \psi_1^0)\right|^2 &= 1/4 \, g_0^2 \, \beta^2 \\
\left|(\psi_3^0 \left| \underset{\wedge}{\mu}_z \right| \psi_4^0)\right|^2 &= 1/4 \, g_0^2 \, \beta^2
\end{aligned} \tag{36}$$

All of these states are non-magnetic, i.e., the matrix elements of the type $(\Psi_i^0 | \underset{\sim}{\mu} | \Psi_i^0)$ vanish. Therefore, a weak applied field has no effect on the zero field energies, to the first order. In fact, as is later pointed out, the application of a weak field (1 to 5 gauss) allows one to find the transitions by applying both a small steady DC field as well as a small audio modulation field of 400 cps. McConnell (18) has shown that these states are magnetic to the second order, but this has little or no effect on the present study.

As in many electron resonance studies, the ever-present problem of relaxation, line width, and saturation were considered. However, no theoretical treatment of these quantities was attempted. Several attempts to derive a line shape function for expected transitions were negative. The application of any Bloch type argument is without justification. It can be stated in advance of the experimental results section, however, that the lines had the usual bell shape encountered in most other EPR studies. One other rather curious effect which will be encountered later is the apparent identity of the dispersion and absorption lines from these samples. No satisfactory explanation of this can be given at the present time. To date no other investigator has observed this somewhat unusual behavior. It must be added that these type transitions are the first truly zero field lines to be observed and perhaps more theoretical studies will follow.

Experimental

1. Chemicals

The malonic acid used was reagent grade and no attempt to further purify it was made. The rather large single crystals were grown from various mixtures of acetone-water (approximately 3:1) and also pure water. A complicating feature of this work was the apparent non-existence of reproducibility in making crystals from the same composition of solution more than once. At first large very regular crystals were obtained from saturated solutions containing approximately a three to one ratio acetone to water; later, better crystals were obtained from pure water. A crystal in order to be large enough to give an appreciable signal to noise ratio had to weigh approximately 1.5 grams.

2. Apparatus

Figure 8 is a block diagram of the apparatus used. The communications receiver is a Hammarlund HQ-160. The phase sensitive detector is a type used by Cole (20). The sample coils used were made of No. 10 silver wire mounted on 1-1/4 inch quartz tubing. The single coil system was selected because of its facility in low temperature measurements. The bridge is also of conventional design (21). The RF source is a General Radio signal generator Type 1001-A. Detailed diagrams of the components used are in Appendix II. Appendix I

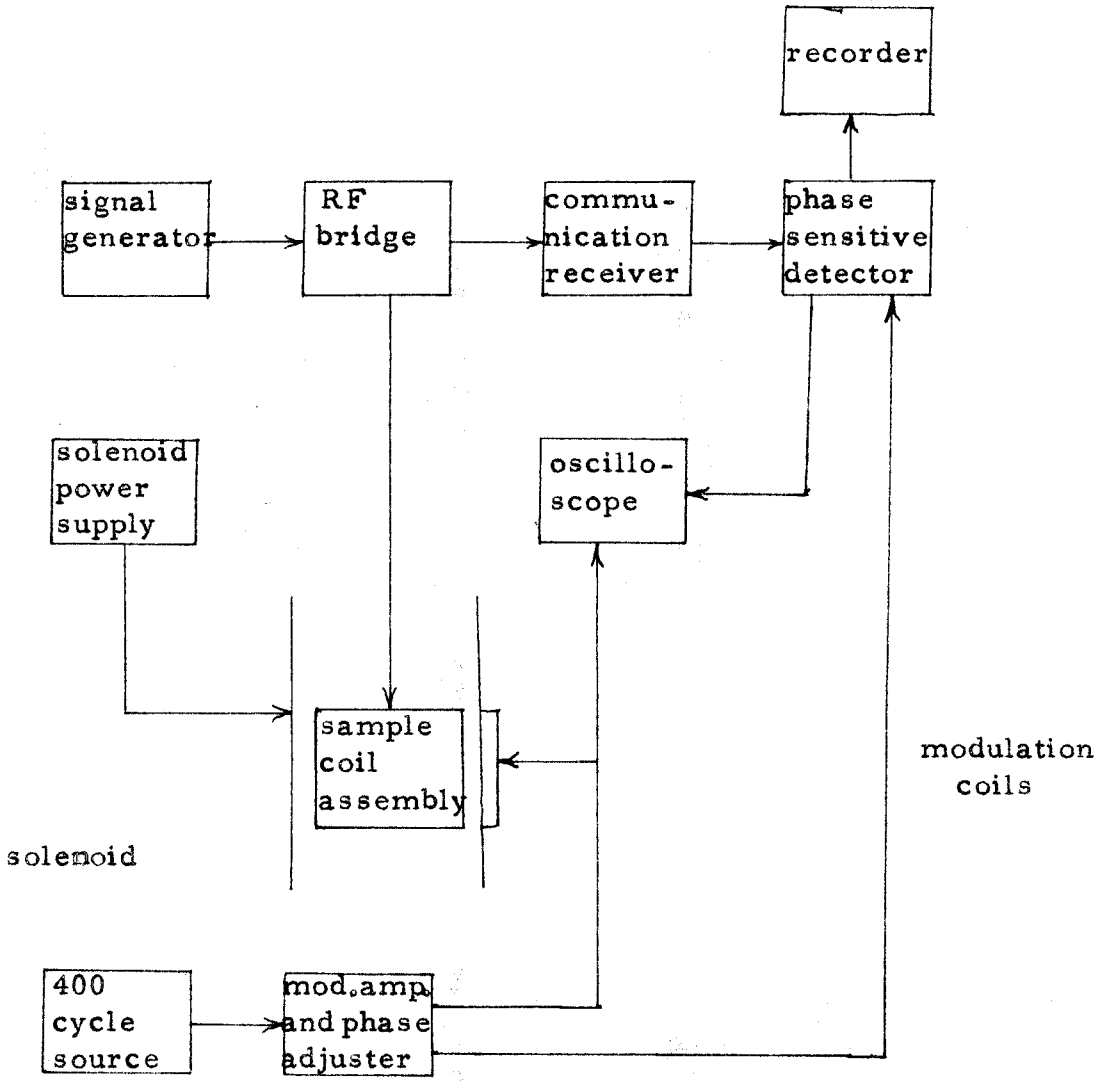

Figure 8. - The block diagram of the apparatus used to observe zero field signals in malonic acid radical.

gives a complete analysis of the asymmetrical bridge and its electrical properties. A thorough understanding of the theory of bridge balance is essential in understanding any resonance phenomena. The bridge was constructed from 1/4 inch aluminum and divided into four sections. These sections are the dummy side, sample side, and the inputs and outputs of each (see Appendix I). The modulation amplifier and phase adjuster was designed to produce a peak to peak 400 cps field of about 4 gauss fed into 20 ohm impedance modulation coil. The phase adjust is necessary to match the phase of signals to the chopper present in the phase sensitive detector. Both recordings and visual plots of the signals were made. The external solenoid used to produce the small DC field was made by wrapping No. 14 copper wire on a six-inch diameter heavy cardboard base and designed to produce a steady field of one gauss per volt applied. It was calibrated using diphenylpicrylhydrazyl (DPPH) and found to be accurate to $\pm$ .1 gauss per volt applied, which is well within the limits of line measurement. Due to a fortunate happenstance, the earth's field in the room where the experiment was made was less than .1 of a gauss and no corrections for it were necessary. The Dewar containing liquid nitrogen, sample coil, and sample wire were inserted into the solenoid and fastened securely. Great care must be taken to avoid any source of microphonics.

The first attempts to locate the resonance were done at room temperature with large irradiated polycrystalline samples. These

experiments all failed. The failure to obtain signals from polycrystalline samples is somewhat puzzling. The samples were of sufficient size to give a signal comparable to that of some single crystals used. The only possible explanation lies in line broadening effects produced by the random orientations of the radicals. Later, large single crystals, also at room temperature, were tried to no avail. Finally, the first signal was found at 15.5 Mcs and 77° K in a single crystal, only in one orientation with respect to the coil axis. Only after finding the right combination of many variables to observe this type resonance was much progress made on completing the over-all experiment. After carefully adjusting the bridge to deliver absorption mode signals, the small steady field is then applied and swept by means of a rheostat. The absorption line was plotted by taking voltage measurements on the solenoid and readings on the output meter of the phase sensitive detector. The apparatus was very sensitive, and 1/4 of a milligram of DPPH could be easily seen at 15 Mcs. The estimated S/N ratio was 100:1. This is roughly equivalent to 5×10^{-6} moles of free spins. Microphonics were a continual source of difficulty, particularly when searching for unknown signals. Whenever careful measurements were to be made, the experiments were always conducted in the evenings, or whenever the building was quiet.

The modulation amplitude was adjusted to gain maximum signal strength. Measurements were made to assure that the line was not

modulation broadened. The phase of the signal was adjusted for maximum output, first with a DPPH sample, then with the sample under study. It was also of considerable importance to check the ease of saturation of the signals. Full output (2 volts) of the signal generator would not saturate the line; this corresponds to a sample coil field of about 20 milligauss. Generally, however, for best signal to noise ratio the output of the signal generator was set to 1 volt.

Several unexpected spurious signals were initially found. First 400 cycle mechanical vibrations produced huge signals in the phase-sensitive detector. These were removed by taking off all mechanical connections between the solenoid and sample assembly. The modulation coil coupled to the solenoid acted like a voice coil and produced these vibrations. Secondly, glass produces a rather strong signal at 77° K and 2.5 gauss in a 15 Mc RF field ($g = 4$). This occurs precisely on the side of the expected zero field line. The coils were later wound on quartz forms, and careful checks were always made to be certain that no signals were obtained with a non-irradiated sample.

3. Samples

The malonic acid crystals were subjected to 50 KV X-rays for about 3 hours each. The X-ray tube had a tungsten target and was operated at 30 ma. The sample was placed approximately 2 inches from the target. The crystals immediately after irradiation were a

flesh color and after several hours turned rather yellow. Some samples were aged as done by McConnell et al. (16) and others investigated right away. No difference was found in the spectra of the samples whether aged or not. The X-band data for these crystals indicate that perhaps another radical is present in significant quantities before aging; however, it did not interfere in these measurements.

Results

Measurements were made on several different crystals and the data were reproducible in every instance. A signal at 15.5 ± .2 Mc was found only along the z direction of the molecular axis. Another signal was found along the molecular y axis at 13.4 ± .2 Mc only. There was no signal found at these frequencies whatsoever when the sample was placed in an orthogonal direction to either of these axes. The four other frequencies predicted could not be found with this apparatus as their predicted values are all above 30 Mc. Work is being conducted now, in this laboratory, to find these other transitions.

The molecular y axis is, within experimental error, parallel to the crystal c axis (16). The c axis was identified visually from a nearly perfect crystal and then checked later by X-band EPR. The molecular z axis was more difficult to locate and was estimated visually and also checked by an X-band measurement. The signal strength was checked versus angular orientation about a given axis and was

found to obey roughly a $\cos^2\theta$ dependence, as predicted. Quantitative measurements could not be made because of poor signal/noise ratio. The two line intensities were, as predicted, equal. The z_1 transition was 15.5 $\pm$ .2 Mc, the predicted value was 15.0 Mc. The y_2 transition was 13.4 Mc, the predicted value was 16.3 Mc. Considering a $\pm$ 2 Mc variance in the values of A, B, and C, this is excellent agreement of experiment and theory.

The same signals could be obtained by balancing the bridge with a 20 gauss steady field applied and then sweeping towards zero field as could be obtained by balancing at zero field and sweeping up. Figure 9 shows the plotted derivative line for both frequencies as they were identical in both width and intensity. Notice the perfect symmetry about zero field.

No satisfactory explanation could be found to unambiguously explain the identity of dispersion and absorption modes.

Since in this experiment the direction of the steady magnetic field is not important, a check to validate this was made. In normal EPR studies the oscillatory magnetic field is placed at right angles to the steady field and the usual "perpendicular" transitions occur. In this experiment the sample coil axis could be placed parallel or perpendicular and the identical line resulted. Of course, the directions could be askew as well. This fact was used to great advantage to show that the transitions are <u>not</u> any normal kind of spin resonance. Several

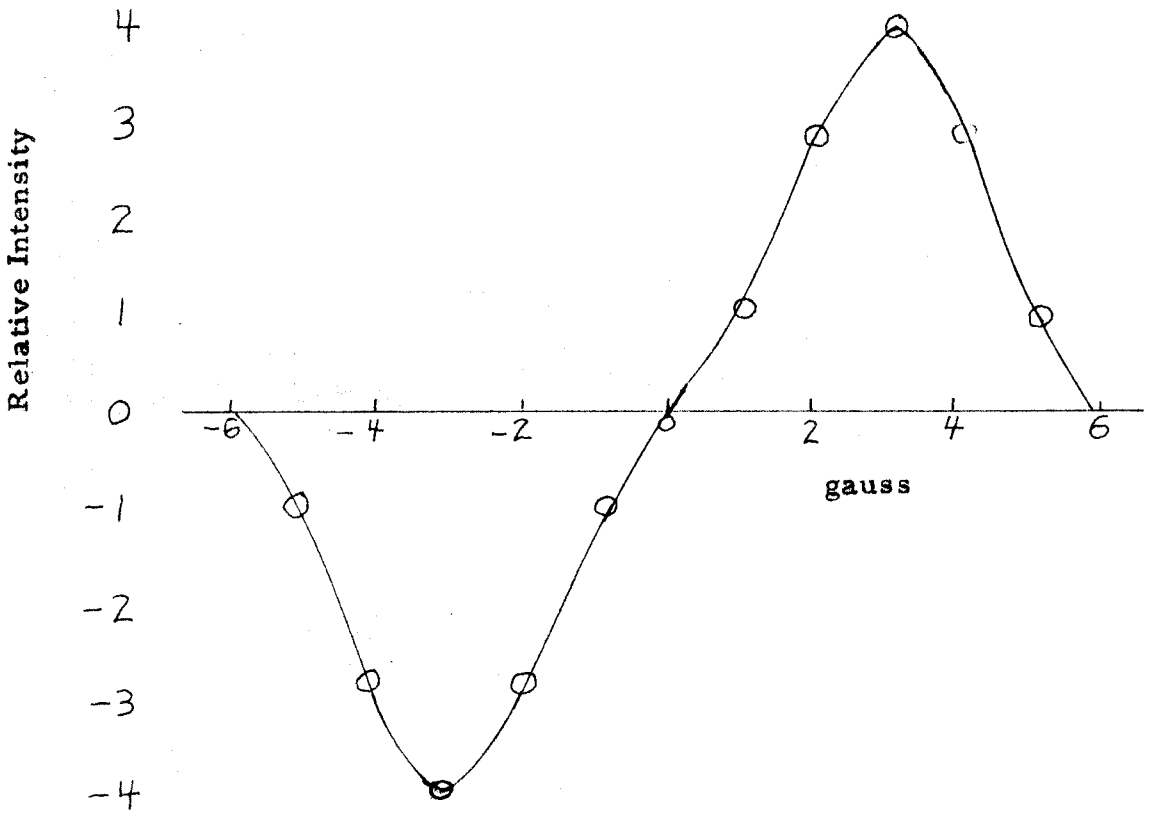

Figure 9. - A plot of the first derivative of the absorption line of malonic acid radical at 15.5 and 13.4 Mc. and 77° K.

checks were made to be certain that the resonances obtained had the abovementioned property. Parallel transitions in a large sample of DPPH at 15 Mc could not be observed under conditions where a perpendicular transition would practically saturate the chopper and produce an overwhelmingly strong signal.

The signal to noise ratio for most samples of the radical when care was taken to avoid any unnecessary microphonics was about 50:1.

The signal strength of the sample at 77° K is roughly equal to 1/8 mg of DPPH at 20° C. Taking into account the Boltzmann factor and also the fact that when looking at one line one "sees" only 1/6 of the sample, the number of radicals produced was estimated to be about one out of every 60,000 molecules present in the crystal.

Conclusion

In conclusion, it should be pointed out that these transitions are the first of their type to be found and the agreement of theory and experiment is excellent. A number of other simple radicals could be easily investigated and the author hopes that subsequent studies are forthcoming. As was suggested (22) the lines may be somewhat broadened by the small applied field and also the modulation field required in order to use the phase-sensitive detector. This, however, is not as yet determined. Attempts are now being made to see these resonances using a quadrupole resonance apparatus of the super-regenerative type where field modulation is not used.

REFERENCES

1. E. R. Andrew, Nuclear Magnetic Resonance (Cambridge University Press, London, 1955).

2. D. J. E. Ingram, Free Radicals (Butterworth's Publications, London, 1958).

3. N. F. Ramsey, Nuclear Moments (Wiley, New York, 1953).

4. J. E. Wertz, Chem. Revs. 55, 829 (1955).

5. B. Bleaney, J. Phys. Chem. 57, 508 (1953).

6. G. E. Pake, Solid State Physics, 2, 1 (1957).

7. H. M. McConnell, Ann. Rev. Phys. Chem. 8, 105 (1957).

8. T. W. Hickmott and P. W. Selwood, J. Chem. Phys. 20, 1339 (1957).

9. R. B. Spooner and P. W. Selwood, J. Am. Chem. Soc. 71, 2184 (1949).

10. S. Meiboom, A. Lowenstein, and S. Alexander, J. Chem. Phys. 29, 969 (1958).

11. H. M. McConnell and D. D. Thompson, J. Chem. Phys. 31, 85 (1959).

12. R. A. Ogg, Jr., Disc. Faraday Soc. 17, 215 (1954).

13. Gutowsky, McCall and Slichter, J. Chem. Phys. 21, 279 (1953).

14. H. M. McConnell, J. Chem. Phys. 28, 430 (1958).

15. L. Giulotto, Nuovo Cimento 5, 498 (1948).

16. McConnell, Heller, Cole, and Fessenden, J. Am. Chem. Soc. (in press).

17. S. I. Weissman, J. Chem. Phys. 22, 1378 (1959).

18. H. M. McConnell, private communication.

19. J. A. Goedkoop and C. H. MacGillavry, Acta Cryst. 10, 125 (1957).

20. T. Cole, Ph. D. Thesis, California Institute of Technology, 1958.

21. H. L. Anderson, Phys. Rev. 76, 1460 (1949).

22. A. F. Hildebrandt, private communication.

APPENDIX I

This appendix is included to give a comprehensive analysis of the asymmetrical bridge used in the apparatus. Refer to the block diagram in Fig. 10 for the following argument.

At balance each T acts independently of the other and therefore one need only consider one T. The output is then regarded as shorted.

$Z_T \equiv e_{in/i3}$ by definition

$$e_{in} = e_1 + e_z = i_1 Z_1 + i_3 Z_3 \tag{1}$$

$$i_z = e_2 / Z_3 \tag{2}$$

where i, e, and z are, respectively, current, voltage, and impedance; combining the three equations above one obtains

$$Z_T = Z_1 + Z_2 + \frac{Z_1 Z_3}{Z_2} \tag{3}$$

now at balance $i_3 = -i'_3$ and therefore

$$e_{in} \left(\frac{1}{Z_T}\right) + \left(\frac{1}{Z'_T}\right) = 0 \tag{4}$$

and

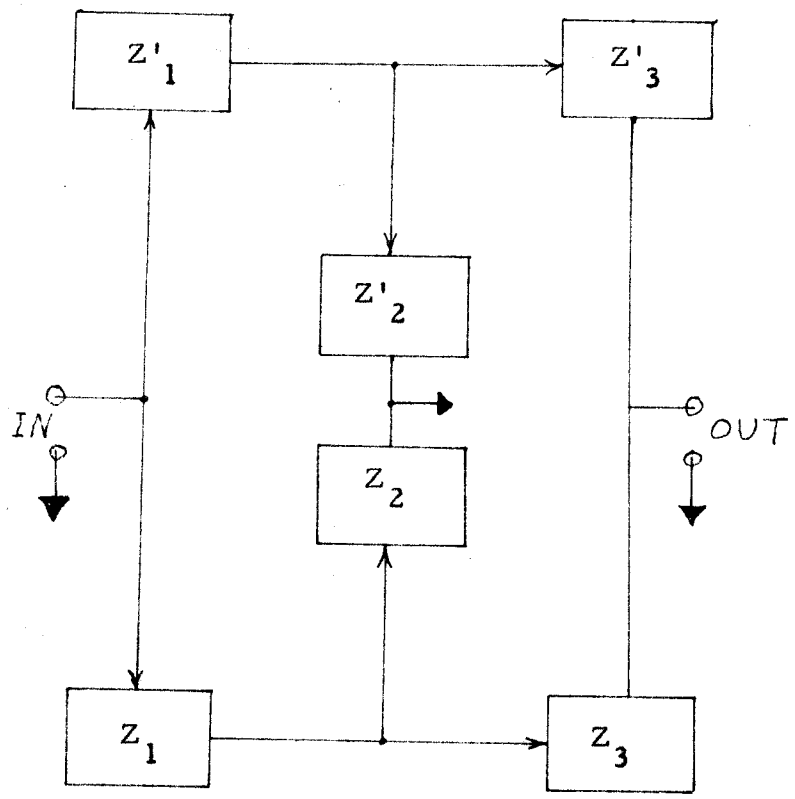

Figure 10. - Block diagram of bridge used in apparatus for zero field measurements.

$$Z_1 + Z_2 + \frac{Z_1 Z_3}{Z_2} + Z'_1 + Z'_2 + \frac{Z'_1 Z'_3}{Z'_2} = 0 \qquad (5)$$

which is the balance equation required. Many choices of impedances are possible but the one actually used is shown in Fig. 11. The choice of variable condensers is an obvious one as they usually are the least troublesome component. The individual impedances are:

$$Z_1 = \frac{1}{i\omega C_1} \qquad Z'_1 = \frac{1}{i\omega C_3}$$

$$Z_2 = \frac{R_L + i\omega L}{(R_L + i\omega L) i\omega C_x + 1} \qquad Z'_2 = \frac{1}{i\omega C_R}$$

$$Z_3 = \frac{1}{i\omega C_2} \qquad Z'_3 = R$$

where R_L is the equivalent series resistance of L, ω is the angular frequency.

Substitution of the individual impedances into the balance equation 5 yields the two balance equations given below:

$$C_x + C_1 C_2 \left(\frac{1}{C_1} + \frac{1}{C_2} + \frac{1}{C_3}\right) - \frac{1}{\omega^2 L} = 0 \qquad (6)$$

$$G_L - R\omega^2 C_1 C_2 \left(1 + \frac{C_R}{C_3}\right) = 0 \qquad (7)$$

where $G_L = \frac{1}{Q\omega L}$ if $Q \gg 1$ and $Q = \frac{\omega L}{R_L}$.

Rewriting equation 7 in the form

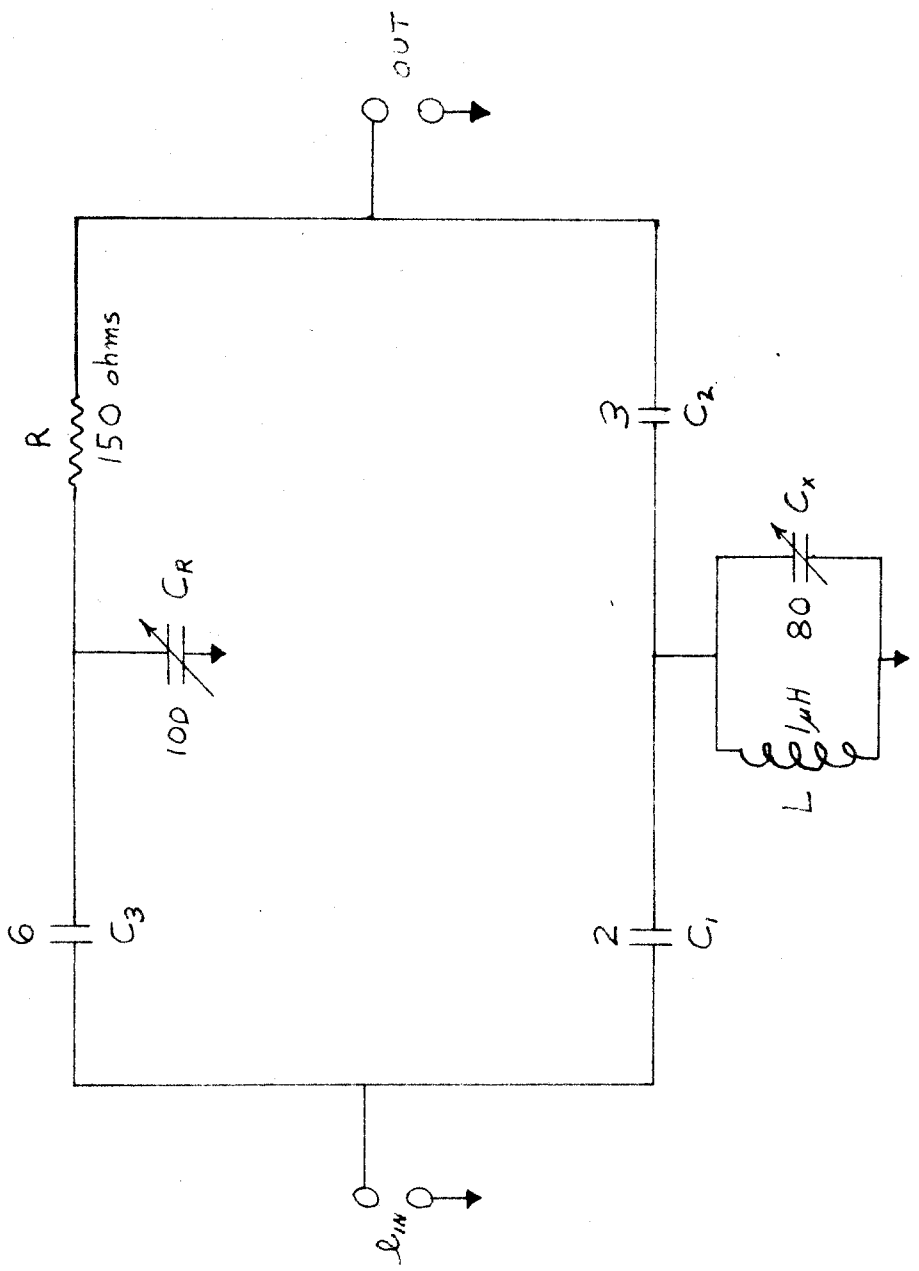

Figure 11. - Schematic of bridge circuit.

$$1 - \omega^3 RQLC_1C_2\left(1 + \frac{C_R}{C_3}\right) = 0 \qquad (8)$$

one sees that the quantity C_R/C_3 must be approximately five in order to obtain an appreciable tuning range. It is important also to keep C_1, C_2, C_3 larger than the stray capacitance of the various leads.

Equation 8 is very useful in determining the Q of the specimen coil. The other quantities are known or can be measured easily. Substitution of the quantities yields a Q for a Ag coil of the type used to be approximately 300. Several coils were used for different size samples to gain the greatest possible filling factor. All of the Q's were about the same value.

It is also of interest to know the current (i_2) through the specimen coil (L) in order to estimate the RF magnetic field present over the sample. At balance

$$i_2 = i_1 - i_3 \qquad (9)$$

and

$$i_2 = \frac{e_1}{Z_1} - \frac{e_{in}}{Z_T} \qquad (10)$$

$$e_{in} = e_1 + e_2 \qquad (11)$$

$$e_2 = i_2Z_2 = i_3Z_3 \qquad (12)$$

therefore

$$i_2 = \frac{e_{in}}{Z_1}\left(1 - Z_{3/Z_T}\right) - \frac{e_{in}}{Z_T} \qquad (13)$$

rearranging

$$i_2 = \left[\frac{Z_T - Z_3 - Z_1}{Z_1 Z_T}\right] e_{in} \qquad (14)$$

from a knowledge of e_{in} and the various Z's, i_2 is easily calculated. For a 10 per cent calculation one may assume that $Z_T \rangle Z_1$, Z_3 and then $i_2 \sim \frac{e_{in}}{Z_1}$. For many cases this is sufficient. The calculated RF field for a 1μ H coil is about 20 milligauss for a 2 volt imput.

APPENDIX II

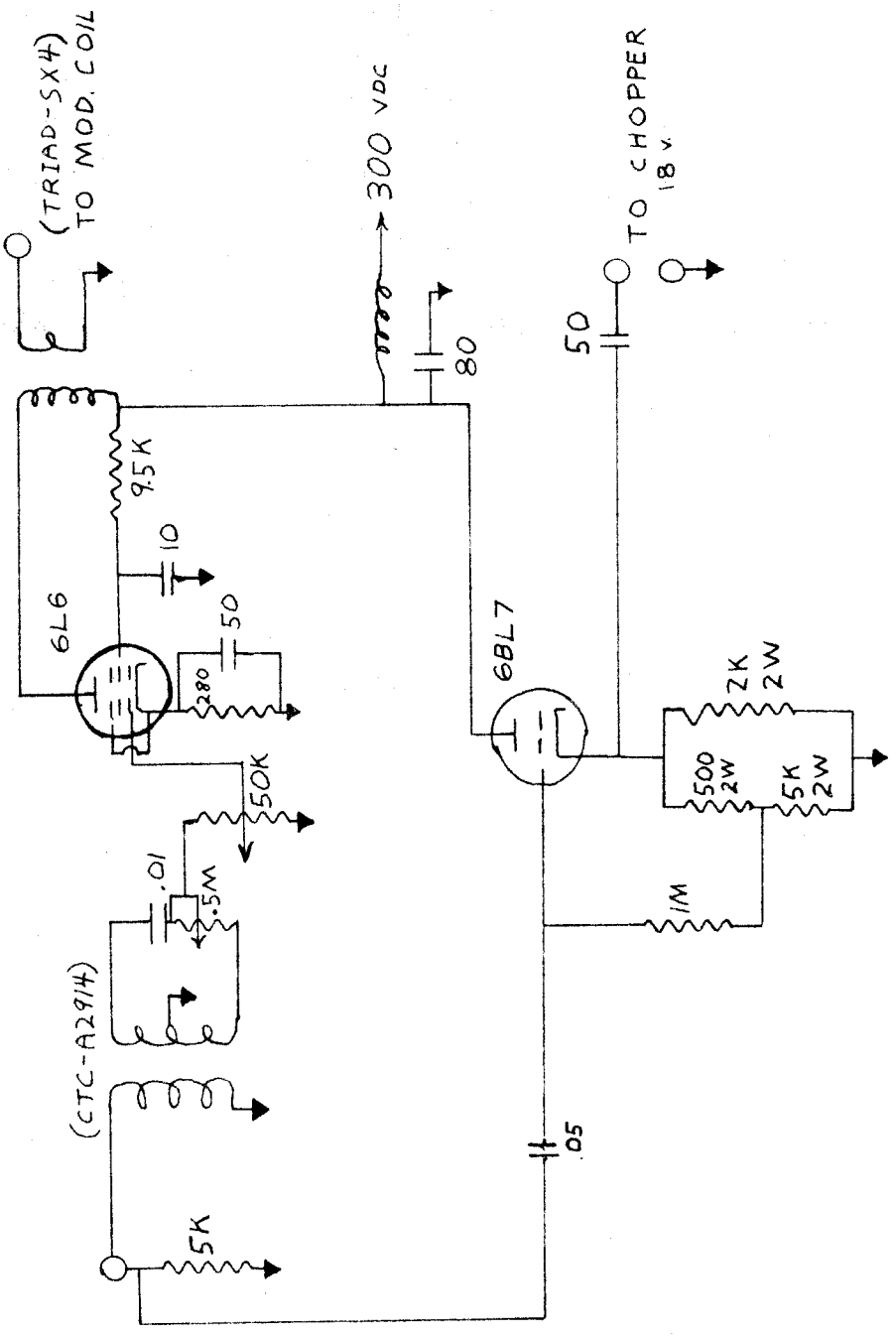

Schematic diagram for the modulation amplifier and phase adjuster.

APPENDIX III

This section gives the details of the T_1 measurements cited in Part I. If the x, y, and z components are included in the Bloch equations, the following expressions result which state the total change of $\underline{M}$ with time. All of the symbols have their usual significance.

$$\begin{aligned}
\dot{M}_x &= \gamma(M_y H_o + M_z H_1 \sin \omega t) - \frac{M_x}{T_2} \\
\dot{M}_y &= \gamma(M_z H_1 \cos \omega t - M_x H_o) - \frac{M_y}{T_2} \qquad (1) \\
\dot{M}_z &= -\gamma(M_x H_1 \sin \omega t + M_y H_1 \cos \omega t) + \frac{(M_o - M_z)}{T_1}
\end{aligned}$$

The method of measuring T_1 is based on the "rapid passage" solution of these equations. The necessary condition for rapid passage is that $T_1, T_2 \gg$ time on resonance $\gg \frac{1}{\gamma H_1}$ and have the spectrometer tuned to receive dispersion mode. The solution of (1) is:

$$M(t) = \int_{-\infty}^{t} \frac{dt' M_o(t) \delta(t')}{T_1(1+\delta^2(t'))^{1/2}} \exp\left[\int_{t}^{t'} \frac{\delta^2(t'') + T_1/T_2 \, dt''}{T_1(1+\delta^2(t''))}\right] \qquad (2)$$

where $\delta = (\omega_0 - \omega)/\gamma H_1$

if $\delta^2 \gg T_1/T_2 \geq 1$ and M_o assumed constant, equation 2 becomes

$$M(t) = \frac{M_o}{T_1} \int_{-\infty}^{\infty} dt' \exp \int_{t}^{t'} \frac{dt''}{T_1} \qquad (3)$$

In the experiment a triangular sweep was employed to sweep through the resonance at $t = 0$ and return in a time t_a. Expressing (3) in these terms, it becomes:

$$M(t) = \frac{M_o}{T_1} \left[\int_{-\infty}^{t_o} \exp \frac{t'-t_o}{T_1} \, dt' - \int_{t_o}^{t_a} \exp \frac{t'-t_o}{T_1} \, dt' \right] \qquad (4)$$

The last term is negative due to the change in sign of δ after passing through resonance. After integration equation 4 becomes:

$$M(t) = \frac{M_o}{T_1} \left(2 - \exp \frac{t}{T_1}\right) \qquad (5)$$

where $t = t_a - t_o$.

At the point where $M(t) \rightarrow 0$

$$T_1 = t/\ln 2 \qquad (6)$$

Equation 6 now allows one to calculate T_1's by measuring the time (t) spent in sweeping triangularly from a point where the signal appears in the up field swing to where it is essentially zero in the down field swing. This method was checked by measuring the T_1 for protons in

pure water and found to be 3.6 ± 0.1 sec, which is in close agreement with literature values. The T_1 used for the calculations in Part I was calculated using this method for the pH = -0.4 solution which is essentially a non-exchanging medium.

PROPOSITIONS

1. Anderson (1) has derived general equations which predict very accurately, by second order perturbation theory, the NMR transition frequencies for systems where the chemical shift (δ) is much larger than the spin-spin coupling (J). It is proposed that this second order effect could be observed in the free precession signal of non-exchanging ammonium ion solution. The second order effect is $\frac{J^2}{\nu_p - \nu_N}$ where ν_p, and ν_N are the earth's field free precession frequencies of a proton and N^{14} nucleus respectively. Where ν_p is 2KC, the second order effect is $\sim$ 1.5 sec^{-1}. This effect cannot be observed at high fields where it becomes vanishingly small.

An extension of Anderson's theory predicts nine proton transitions in the earth's field spectrum.

2. A more sensitive "Pound-Watkins" (2) type NMR probe using FM detection is proposed. This allows reception of dispersion mode only, but for many studies this is of no consequence. The usual P-W circuit uses AM detection.

3. In certain resonance studies it is sometimes advantageous to sweep frequency instead of field; however, no spectrometer of this type has yet been perfected which matches the efficiency of constant frequency units. A simple automatic tracking bridge is proposed.

4. Pastor and Turkevich (3) found an inverse linear relationship between the chemical resonance energy of some polynuclear aromatic hydrocarbons and the EPR line widths of their respective negative ions as formed by potassium in dioxane. The agreement of their experimental results must be fortuitous. The main line narrowing process in these systems is known to be intermolecular electron exchange.

5. A novel scheme whereby one may observe free precession of one nucleus in the field of another is proposed. By compensating for the earth's field, and placing a large ($\sim$ 7 kilograms) magnetic field on a sample where a large spin-spin coupling (J) exists between two nuclei, such as is present in PF_3, a signal should be observed as the F^{19} magnetization decays in the field produced at that nucleus by P^{31}. The complete Hamiltonian for that system is:

$$H = J\, I_1 \cdot I_2$$

The eigenenergies in zero applied field are simply:

$$\frac{J}{2}\ [\, F(F+1)-I_1(I_1+1)-I_2(I_2+1)]$$

where

$$F = I_1+I_2$$

The allowed transitions occur between the states where $\Delta F = 1$. For PF_3 they are at 2J and J, corresponding to frequencies 2.8 and 1.4 KC. This effect may be observed in many other compounds where

J is large and the thermal and spin-spin relaxation times are $\sim$ 1 second or longer.

6. Investigators at Duke University have published numerous papers on the EPR spectra of organic radicals produced by X-rays at 77° K. One of these studies (5) proposed that the probable specie present after irradiating dimethyl mercury and similar compounds was the radical-ion $(C_2H_4)^+$. From the published width of this spectrum (which looks like one of four equally coupled protons), it is impossible that this specie be responsible for the observed data.

7. An NMR study of liquid iodine heptafluoride (6) is proposed in order to further substantiate its molecular structure. The two main possibilities for its structure are a pentagonal based bipyramid and a plane. An NMR spectrum would differentiate between the two possibilities.

8. An EPR analysis of the hydroxy dimesityl methyl radical is proposed which would ascertain if the very small isotropic coupling of hydroxy protons in methanol type radicals is due to coplanarity.

9. Theory predicts that benzyl radical has negative spin density in the meta position (7). An experiment involving X-irradiated p-toluic acid is proposed to test this hypothesis. If the absolute sum of the

spin densities is greater than unity the radical would have negative spin densities. A study of a single crystal could yield quantitative data.

10. It is proposed that the Chemistry Department require all first year graduate students to take a course in experimental electronics. This course should be designed to facilitate the students' mastery of the maze of new electronic devices currently used in modern chemistry.

REFERENCES FOR PROPOSITIONS

1. W. A. Anderson, Phys. Rev., 102, 151 (1956)

2. G. D. Watkins, Thesis, Harvard University, 1952

3. R. C. Pastor and J. Turkevich, J. Chem. Phys. 23, 1731 (1955).

4. W. Gordy, J. Am. Chem. Soc. 78, 3243 (1956).

5. Lord, Lynch, Schumb, and Slowinski, J. Am. Chem. Soc. 72, 522 (1950).

6. H. H. Dearman, private communication.